



Significance of the longitudinal component of paraxial light in position-dependent selection rules for quadrupole atomic transitions

ABDULLAH F. ALHARBI,^{1,*} ANDREAS LYRAS,² AND VASSILIS E. LEMBESSIS² 

¹King Abdulaziz City for Science and Technology (KACST), Riyadh 11442, Saudi Arabia

²Quantum Technology Group, Department of Physics and Astronomy, College of Science, King Saud University, Riyadh 11451, Saudi Arabia

*harbi@kacst.edu.sa

Abstract: It is well established that the longitudinal component of paraxial optical vortices has a key role in specific atomic quadrupole transitions near the beam axis when the spin and orbital angular momenta are antiparallel. By deriving analytical expressions for the position-dependent selection rules, this work shows that the significant role of the longitudinal fields is not limited to this case, but rather is a more general feature for any paraxial light including, for example, optical vortices with parallel spin and orbital angular momenta as well as Gaussian beams. Numerically, the transition strengths induced by the weaker longitudinal component can be twice as high as those by the stronger transverse component. We also show that there are transitions that can be induced exclusively by the longitudinal component for light carrying two quanta of orbital angular momentum.

© 2023 Optica Publishing Group under the terms of the [Optica Open Access Publishing Agreement](#)

1. Introduction

A new class of light beams known as vortex beams or twisted light has attracted significant interest due its unique and novel characteristics [1,2]. These beams such as Bessel beams and Laguerre – Gauss beams can carry Spin Angular Momentum (SAM), associated with circular polarization, and Orbital Angular Momentum (OAM), associated with helical wave front, with quantized amounts of $\sigma\hbar$ and $\ell\hbar$ per photon, respectively. Here $\sigma = 1(-1)$ for left (right) circular polarization while the topological charge ℓ is an integer which can either be positive or negative. In addition to boosting communication capacity in classical and quantum communications [3,4], light with OAM is also exploited for various light-matter interactions. It can be, for example, used in guiding geometries, mechanical rotation and trapping of atoms [5–7]. Moreover, the transfer of optical OAM can modulate the atomic internal state. This latter effect can convey novel features for quantum information related applications such as preparing long-lived qubits and suggesting novel ways to implement quantum memories and/or quantum repeaters. However, a comprehensive study of this recent type of light-matter interaction is necessary to lay the foundations for advancing these applications.

Substantial progress in this field was achieved by recent breakthrough experiments which elucidated the selection rules for atomic transitions induced by OAM-carrying beams [8,9]. The derivation of the angular-momentum selection rules for the twisted-light-photoexcitation near the phase singularity is outlined using different approaches in [10] and [11]. To treat the more general case where the atom is located at an arbitrary distance from the vortex core, one may express the vector potential of the vortex beam as a superposition of plane waves. This expansion reduces the computation of twisted-photon matrix elements to those of plane wave matrix elements. Although this method applied in [9,12–14] is powerful, it obscures some critical information about the contribution of different components of the field.

An alternative approach is based on the Power-Zienau-Woolley (PZW) formalism [15–17] where the coupling of the atom to the electric field is written in the form of a multipolar series expansion about the center of mass coordinates. This approach was employed in [18] with a purely-transverse form of the electric field of a Laguerre-Gaussian (LG) beam. It is a common practice to assume that propagating fields are purely transverse for parameters such that the paraxial approximation is applicable [19]. However, it was shown that, even in this domain of parameters, the field components parallel to the propagation direction have important measurable effects on quadrupole transitions for a specific combination of spin and orbital angular momenta (antiparallel configuration) at a specific location (the center of the beam) [8,10]. In a recent work, these effects were also shown to be present in a broader family of optical vortices [20]. The longitudinal field components have been studied in the past by several researchers [21] but the interest in them and their effects has been rekindled the recent years after the work of Bliokh [22]. Subsequent efforts have extended the study of the longitudinal field components in various types of structured-light beams, placing emphasis on the effects of these components on the optical properties of the particular beams [23]. Moreover, a number of studies demonstrated novel effects induced by the longitudinal field components [24] in, for example, two-level atom dynamics [25] and cold atoms trapping [26].

This work studies twisted light absorption by a bound electron involving different variations in magnetic quantum number Δm and shows how the selection rules depend on position using the above mentioned approach. Here we take into account the full spatial dependence of the electric field including the longitudinal component in order to demonstrate the role of this component in different cases of beam configurations with different combinations of SAM and OAM.

2. Quadrupole interaction Hamiltonian

The multipolar Hamiltonian series expansion about the atom's center of mass coordinates $\mathbf{r} = (x, y, z)$ can be expressed as follows:

$$H_{int} = H_{dp} + H_{qd} + \dots \quad (1)$$

where H_{dp} and H_{qd} represent the electric dipole and quadrupole interactions, respectively. The latter term H_{qd} is given by:

$$H_{qd} = -\frac{1}{2} \sum_{ij} Q_{ij} \nabla_i E_j \quad (2)$$

where E_j are the electric field components along x, y and z directions. $Q_{ij} = e x'_i x'_j$ are the quadrupole transition operators with x'_i the components of the internal position vectors.

To derive the expression of the electric field, we first write the vector potential $\mathbf{A}_{\ell p}$ for circularly polarized LG beams, parameterized by two indices, the azimuthal mode index ℓ and the radial mode index p , in the following form:

$$\mathbf{A}_{\ell p} = \frac{(\hat{x} + i\sigma\hat{y})}{\sqrt{2}} A_0 u(\mathbf{r}) e^{(-i\omega t + ikz)} + c.c., \quad (3)$$

where $u(\mathbf{r}) = u_1(\mathbf{r}) u_2(\mathbf{r})$ is the mode function. $u_1(\mathbf{r})$ describes the part of the mode function that depends on ℓ and p :

$$u_1(\mathbf{r}) = \sqrt{\frac{p!}{(|\ell| + p)!}} \left(\frac{\sqrt{2}\rho}{w(z)} \right)^{|\ell|} \mathcal{L}_p^{|\ell|} \left(\frac{2\rho^2}{w_0^2} \right) \times \exp \left(i\ell\varphi - i(2p + |\ell|) \arctan\left(\frac{z}{z_R}\right) \right) \quad (4)$$

while $u_2(\mathbf{r})$ is the part of the mode function related to the ordinary Gaussian beam:

$$u_2(\mathbf{r}) = \frac{w_0}{w(z)} \exp\left(\frac{-\rho^2}{w(z)^2} + \frac{ik\rho^2}{2R(z)^2} - i \arctan\left(\frac{z}{z_R}\right)\right) \quad (5)$$

where z is the axial distance from the beam's focus (or "waist"), ρ is the radial distance from the center axis of the beam, A_0 the vector potential at the origin ($\rho = 0, z = 0$), $w(z)$ is the radius at which the field amplitudes fall to $1/e$ of their axial values, $w_0 = w(0)$ is a waist radius, $\mathcal{L}_p^{|\ell|}(\frac{2\rho^2}{w_0^2})$ is an associated Laguerre polynomial, z_R is the Rayleigh length, $R(z)$ is the radius of curvature of the beam's wavefronts at z . This particular factorization of the overall mode function will be useful in classifying the contribution to transition amplitudes of the longitudinal field components for various beam types including the purely Gaussian beam.

Using $\mathbf{A}_{\ell p}$ and the scalar potential Φ obtained from the Lorenz condition ($\nabla \cdot \mathbf{A} = -\frac{1}{c^2} \frac{\partial \Phi}{\partial t}$), the electric field \mathbf{E} , at an approximation consistent with the paraxial approximation [27], can be written as:

$$\begin{aligned} \mathbf{E}^{(+)}(\mathbf{r}) &= E_x \hat{\mathbf{x}} + E_y \hat{\mathbf{y}} + E_z \hat{\mathbf{z}} \\ &= \frac{E_0}{\sqrt{2}} e^{ikz} [(\hat{x} + i\sigma \hat{y}) u(\mathbf{r}) \\ &\quad + \hat{z} \frac{i}{k} (\frac{\partial u(\mathbf{r})}{\partial x} + i\sigma \frac{\partial u(\mathbf{r})}{\partial y})] \end{aligned} \quad (6)$$

where $E_0 = -i\omega A_0$ is defined using the average power of the beam P by the relation [28]: $P = (\pi\epsilon_0 c w_0^2/4) |E_0|^2$. The transition matrix element for transition from an initial state $|i\rangle$ to a final state $\langle f|$ through the quadrupole coupling (2) is:

$$\langle f|H_{qd}|i\rangle = -\frac{1}{2} \sum_{ij} \langle f|Q_{ij}|i\rangle \nabla_i E_j. \quad (7)$$

3. Results and discussion

Expanding the quadrupole operators in Eq. (7) in terms of spherical tensors, one can have a grasp as to when the longitudinal fields of the field affect quadrupole transitions. It should be noted here that tensors of the form T_n^2 result in transitions with $\Delta m = n$. The expansion of the operators Q_{iz} have no $T_{\pm 2}^2$ components and, hence, the longitudinal component of any form of light play no role in quadrupole transitions with $\Delta m = \pm 2$. To work out other channels, we write the interaction matrix in terms of spherical tensors:

$$\begin{aligned} \langle f|H_{qd}|i\rangle &= -\sqrt{\frac{\pi}{10}} e E_0 e^{ikz} u(\mathbf{r}) \\ &\times \left\{ M_T^+ \langle r^2 T_2^2 \rangle + M_T^- \langle r^2 T_{-2}^2 \rangle \right. \\ &+ (N_T^+ + N_L^+) \langle r^2 T_1^2 \rangle + (N_T^- + N_L^-) \langle r^2 T_{-1}^2 \rangle \\ &\left. + (O_T + O_L) \langle r^2 T_0^2 \rangle \right\} \end{aligned} \quad (8)$$

where the functions M^\pm , N^\pm and O are as follows:

$$\begin{aligned}
 M_T^\pm &= \frac{1}{\sqrt{6}} e^{-i\sigma\varphi} (1 \pm \sigma) \left(\frac{|\ell| + \sigma\ell}{\rho} + \frac{1}{\mathcal{L}} \frac{\partial \mathcal{L}}{\partial \rho} - \frac{2\rho}{w_0^2} \right) \\
 N_T^\pm &= -\frac{1}{\sqrt{6}} (\sigma \pm 1) ik \\
 N_L^\pm &= \frac{1}{\sqrt{6}} (NG_L^\pm + NL_L^\pm) \\
 O_T &= \frac{1}{2} O_L = e^{i\sigma\varphi} \left(\frac{|\ell| - \sigma\ell}{\rho} + \frac{1}{\mathcal{L}} \frac{\partial \mathcal{L}}{\partial \rho} - \frac{2\rho}{w_0^2} \right)
 \end{aligned} \tag{9}$$

and

$$\begin{aligned}
 NG_L^\pm &= \frac{i}{k} e^{i(\sigma \pm 1)\varphi} \left\{ (\sigma \pm 1) \frac{2}{w_0^2} \mp \frac{4\rho^2}{w_0^4} \right\} \\
 NL_L^\pm &= \frac{i}{k} e^{i(\sigma \pm 1)\varphi} \left\{ \frac{(|\ell| - \sigma\ell)(\mp|\ell| - \ell - \sigma \pm 1)}{\rho^2} \right. \\
 &\quad \left. + \frac{2}{w_0^2} (\pm 2|\ell| \mp \sigma\ell + \ell) \right. \\
 &\quad \left. + \frac{1}{\mathcal{L}} \frac{\partial \mathcal{L}}{\partial \rho} \left(\frac{\mp|\ell| - \ell - \sigma \pm \sigma\ell}{\rho} \right) \right. \\
 &\quad \left. \pm \frac{4\rho}{w_0^2} \right\} \mp \frac{1}{\mathcal{L}} \frac{\partial^2 \mathcal{L}}{\partial \rho^2} \left. \right\}
 \end{aligned} \tag{10}$$

Here, we dropped the position dependence and super- and subscripts from $\mathcal{L}_p^{|\ell|} \left(\frac{2\rho^2}{w_0^2} \right)$ for notational clarity. From the above expressions, it becomes clear that the transition matrix elements are proportional to the beam profile multiplied by radially varying factors that are determined by the beam parameters, in particular σ , ℓ , ρ and w_0 . In the following, we discuss the effects of these factors on quadrupole transitions with selection rules $\Delta m = \pm 2, \pm 1, 0$:

i) $\Delta m = \pm 2$

The form of M_T^\pm suggests that the spin σ controls completely the transition between states with $\Delta m = \pm 2$, i.e. left(right)-handed circularly polarized light can only induce $\Delta m = 2\sigma$ transitions. M_T^\pm is composed of three terms. The first term survives only if ℓ is nonzero and has the same sign of σ while the second one contributes only if $\rho \neq 0$. In contrast to the first two terms, the last one originates from the gradient of the gaussian mode function u_2 . Given that the first term is inversely proportional to ρ , it has non-zero contribution near the beam axis only if $\ell = \sigma = \pm 1$. On the other hand, the other terms always yield null at this point.

ii) $\Delta m = \pm 1$

There are two factors governing $\Delta m = \pm 1$ transitions: N_T^\pm that depends only on the dominant transverse component of the field and N_L^\pm that originates from the longitudinal component. N_T^\pm leads to transitions obeying the selection rule $\Delta m = \sigma$ with an absolute value of $\frac{2}{\sqrt{6}}k$. On the other hand, the factor N_L^\pm is composed of two parts: NG_L^\pm and NL_L^\pm which are related to the presence of u_1 and u_2 functions in the field, respectively. Both terms in NG_L (that do not depend on the beam's angular momentum) are typically weak since they are proportional to w_0^{-2} and w_0^{-4} , respectively. It is interesting to note that the first term in NG_L^\pm results in transitions satisfying the rule $\Delta m = \sigma$, and, thus, its weak

contribution is buried under the dominant contribution of N_T^\pm . The second term in NG_L^\pm is present for both cases of $\Delta m = \pm 1$ and scales with ρ^2 , so its slight effects can be detected away from the phase singularity.

On the other hand, the first term in NL_L^\pm is nonzero only when the spin and orbital angular momenta are antiparallel to each other. As a result, the second bracket in this term can be rewritten as $\mp 2(|\ell| - 1)$. This means that this channel is completely suppressed for $|\ell| = 1$ and makes the cases with $|\ell| = 2$ interesting to explore. On the other hand, the second term in NL_L^\pm contributes to all cases of ℓ . However, they have always zero magnitude near the phase singularity since they have the same spatial dependence of the beam profile. The last terms are dependent on the position derivative of \mathcal{L} and, hence, are zero for $p = 0$.

iii) $\Delta m = 0$

For the case of $\Delta m = 0$ transitions, Quinteiro et al [10,20] showed that the longitudinal component of paraxial vortices has an important role in atomic quadrupole transitions near the beam axis when SAM and OAM are antiparallel. The result of $O_T = \frac{1}{2} O_L$ shows clearly that this property is not limited to this special case. Instead, it is appreciable for all paraxial beams including optical vortices with parallel momenta and Gaussian beams. Numerically, the transition strengths induced by the weaker longitudinal component are exactly double the rates due to the stronger transverse component. Similar to M_T^\pm , both the factors O_T and O_L are composed of three terms. The only difference is that the middle sign in the first term is negative which means that it is non zero only if ℓ is nonzero and has the opposite sign of σ . This term, which is inversely proportional to ρ , causes a transition near the phase singularity only if $\ell = -\sigma$, which is the case reported in [10,20].

As an application, we now study the transition strengths Ω for $LG_{0,1}^1$ and Gaussian modes as a function of the distance from the beam center, results shown in Fig. 1. The presented strengths are obtained by multiplying the transition amplitudes absolute squared by the same overall factor to facilitate easy comparison with those measured in [9]. In that experiment, the measurements were conducted for quadrupole transitions between the Zeeman split magnetic levels of $4S_{1/2}$ to those of $3D_{5/2}$ in a single $^{40}\text{Ca}^+$ ion. The ion was placed in a Paul trap with sub-wavelength positioning resolution. In our study, we used the same width of the beam waist used in [9] with $w_0 = 4\lambda$, where $\lambda = 0.729 \mu\text{m}$.

The approximation of a full transverse field is plotted in Fig. 1 in dotted red while the corrected description including the longitudinal field is in solid black. In general, the latter curves agree with those obtained by another method used to model the experimental data in [9]. The advantage of our work is that it yields the transition amplitudes in the form of analytical expressions and provides the exact weight of the different field components in the transition amplitudes. A first remark from the plots is that the rule $\Delta m = \sigma + \ell$ is always fulfilled at the beam center for all transverse and longitudinal fields. However, this conservation rule is usually violated when the atom is positioned away from this center. The underlying physics of these observations, as explained in details in [29], is that SAM is always $\sigma\hbar$ per photon irrespective of the displacement of the calculation axis with respect to the beam axis (z -axis). On the other hand, OAM for a mode is only well defined about the beam axis. When the calculation axis is laterally displaced, this mode is expressed as a superposition of OAM modes. As a result, an atom that is on a parallel axis to the beam axis can absorb a photon carrying any possible amount of OAM ($\ell\hbar$) within this superposition. This is why, for example, a Gaussian mode that carries an angular momentum of only $\sigma\hbar$ can drive electric quadrupole transitions such that $\Delta m \neq \sigma$ in an atom placed at a distance from the beam center.

It is clear that for all seven cases for $\Delta m = \sigma$ (the first three plots in the first column and the last four plots in the third column), there is no discrepancy between the two treatments. On the other hand for transitions with $\Delta m = -\sigma$ (the last four plots in the first column and the first three

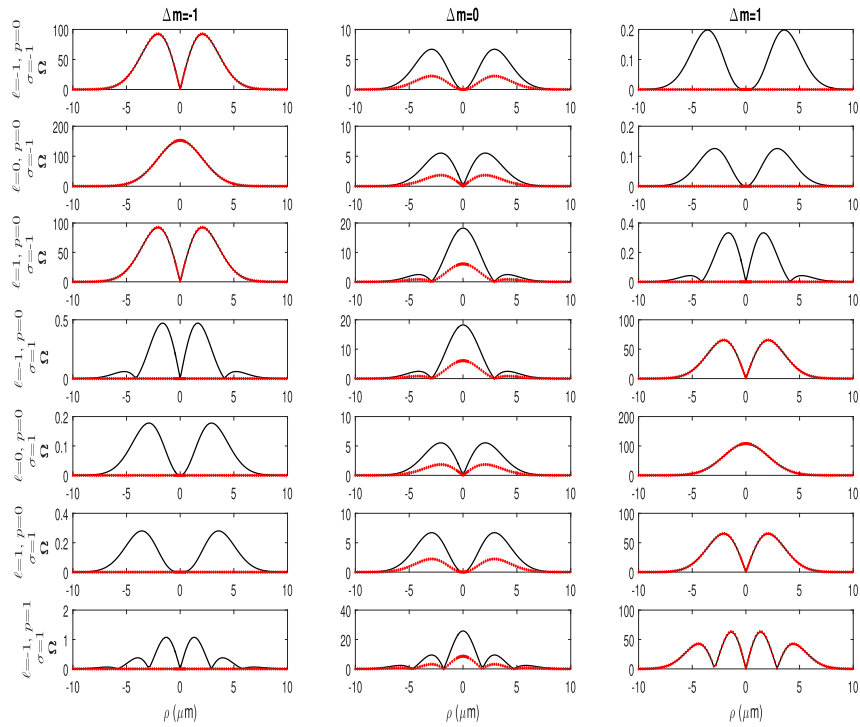


Fig. 1. Transition strengths for quadrupole transitions between the Zeeman split magnetic levels of trapped $^{40}\text{Ca}^+$ ion as a function of the distance from the beam center. The contributions to the transition strengths from the transverse field component only (red dotted) and the complete field including the longitudinal component (solid black) are plotted for different combinations of $\ell = -1, 0, 1$, $\sigma = -1, 1$ and $p = 0, 1$.

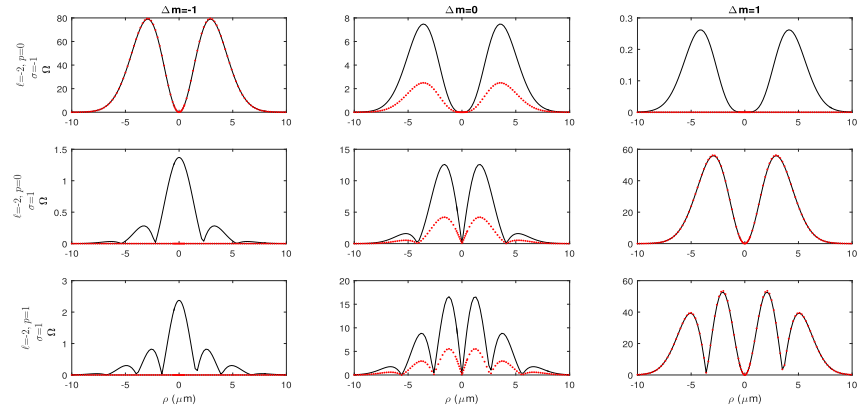


Fig. 2. Same as Fig. 1, but for different combinations of $\ell = -2$, $\sigma = -1, 1$ and $p = 0, 1$.

plots in the third column), there is no contribution comes from the transverse field while the contribution of the longitudinal field is weak. This effect comes exclusively from the Gaussian mode function (u_2) and can be detected experimentally only if the polarization of the beam is pure. Otherwise, the measured data would be contaminated by the signal induced by the small portion of the beam with the opposite spin. The middle column in Fig. 1 confirms that the role of

the longitudinal fields are appreciable for all cases including vortex beams with parallel spin and orbital angular momenta as well as Gaussian beams. The results of LG beams with $p = 1$ (last row) closely resemble that of the case of $p = 0$ (fourth row). However, the latter have more nodes with relatively higher transition strengths at a larger distance from the center.

Similarly, Fig. 2 disentangles the contributions of the electric field components to the transition strengths but for different combinations of $\ell = -2$ and $\sigma = -1, 1$. A striking remark about the case of $|\ell| = 2$ compared to $|\ell| = 1$ is that the first term in NL_L is nonzero when the signs of the spin and orbital angular momenta are opposite. Therefore, it induces $\Delta m = -1$ transitions near the phase singularity while the contribution of the stronger transverse component is completely turned off (see the first plots in the middle and bottom rows).

4. Conclusion

According to Lax et al [30], the purely transverse field forms the zeroth order solution in $1/kw_0$ of the wave equation in free space. It is common to assume LG propagating fields purely transverse when the paraxiality condition $((2p + |\ell| + 1)/(\lambda w_0))^2 \ll 1$ is fulfilled [19]. However, it has been demonstrated that the longitudinal component of paraxial LG beams have non-negligible effects close to the beam axis when the two angular momenta are opposite to each other ($\ell = -\sigma$) with parameters such that $w_0 \approx 4\lambda$. Our analysis shows that the importance of this component extends to a large number of previously unknown cases of quadrupole transitions induced by paraxial light beams. In particular, we have found clearly that the influence of the longitudinal fields is fingerprinted in all position-dependence transitions with $\Delta m = 0$ and $\Delta m = -\sigma$ for all types of studied beams. We have also identified specific transitions for which this contribution is the only way that they can be excited. The case of atomic interaction with beams carrying OAM of $\pm 2\ell\hbar$ is very interesting to further investigate, particularly in terms of magnetic dipole transitions which, in principle, could be comparable to those excited through electric quadrupole.

Funding. King Abdulaziz City for Science and Technology (NSTIP: 2-17-01-001-0057).

Acknowledgment. The project was funded by the National Science, Technology and Innovation Plan (NSTIP), King Abdulaziz City for Science and Technology, Kingdom of Saudi Arabia, Award number (2-17-01-001-0057).

Disclosures. The authors declare no competing interests.

Data availability. Data underlying the results presented in this paper are not publicly available at this time but may be obtained from the authors upon reasonable request

References

1. L. Allen, M. W. Beijersbergen, R. J. C. Spreeuw, *et al.*, "Orbital angular momentum of light and the transformation of Laguerre-Gaussian laser modes," *Phys. Rev. A* **45**(11), 8185–8189 (1992).
2. S. Franke-Arnold, "30 years of orbital angular momentum of light," *Nat. Rev. Phys.* **4**(6), 361 (2022).
3. L. A. Rusch, M. Rad, K. Allahverdyan, *et al.*, "Carrying data on the orbital angular momentum of light," *IEEE Commun. Mag.* **56**(2), 219–224 (2018).
4. M. Krenn, J. Handsteiner, M. Fink, *et al.*, "Twisted light transmission over 143 km," *Proc. Natl. Acad. Sci.* **113**(48), 13648–13653 (2016).
5. S. Franke-Arnold, "Optical angular momentum and atoms," *Philos. Trans. R. Soc., A* **375**(2087), 20150435 (2017).
6. A. M. Yao and M. J. Padgett, "Orbital angular momentum: origins, behavior and applications," *Adv. Opt. Photonics* **3**(2), 161–204 (2011).
7. M. J. Padgett, "Orbital angular momentum 25 years on," *Opt. Express* **25**(10), 11265–11274 (2017).
8. C. T. Schmiegelow, J. Schulz, H. Kaufmann, *et al.*, "Transfer of optical orbital angular momentum to a bound electron," *Nat. Commun.* **7**(1), 12998 (2016).
9. A. Afanasev, C. E. Carlson, C. T. Schmiegelow, *et al.*, "Experimental verification of position-dependent angular-momentum selection rules for absorption of twisted light by a bound electron," *New J. Phys.* **20**(2), 023032 (2018).
10. G. F. Quinteiro, F. Schmidt-Kaler, and C. T. Schmiegelow, "Twisted-light-ion interaction: The role of longitudinal fields," *Phys. Rev. Lett.* **119**(25), 253203 (2017).
11. A. F. Alharbi, A. Lyras, V. E. Lembessis, *et al.*, "Photoexcitation of atoms near the center of vortex light," *Results Phys.* **46**, 106311 (2023).

12. H. M. Scholz-Marggraf, S. Fritzsche, V. G. Serbo, *et al.*, "Absorption of twisted light by hydrogenlike atoms," *Phys. Rev. A* **90**(1), 013425 (2014).
13. A. A. Peshkov, D. Seipt, A. Surzhykov, *et al.*, "Photoexcitation of atoms by Laguerre-Gaussian beams," *Phys. Rev. A* **96**(2), 023407 (2017).
14. G. F. Quinteiro, A. O. Lucero, and P. I. Tamborenea, "Electronic transitions in quantum dots and rings induced by inhomogeneous off-centered light beams," *J. Phys.: Condens. Matter* **22**(50), 505802 (2010).
15. E. A. Power and S. Zienau, "Coulomb Gauge in Non-Relativistic Quantum Electro-Dynamics and the Shape of Spectral Lines," *Philos. Trans. R. Soc., A* **251**(999), 427–454 (1959).
16. R. G. Woolley, "Molecular Quantum Electrodynamics," *Proceedings of the Royal Society of London Series A* **321**, 557–572 (1971).
17. V. E. Lembessis and M. Babiker, "Enhanced quadrupole effects for atoms in optical vortices," *Phys. Rev. Lett.* **110**(8), 083002 (2013).
18. S. Bougouffa and M. Babiker, "Quadrupole absorption rate and orbital angular momentum transfer for atoms in optical vortices," *Phys. Rev. A* **102**(6), 063706 (2020).
19. P. Vaveliuk, B. Ruiz, and A. Lencina, "Limits of the paraxial approximation in laser beams," *Opt. Lett.* **32**(8), 927–929 (2007).
20. G. F. Q. Rosen, "On the importance of the longitudinal component of paraxial optical vortices in the interaction with atoms," *J. Opt. Soc. Am. B* **40**(4), C73–C77 (2023).
21. K. A. Forbes, D. Green, and G. A. Jones, "Relevance of longitudinal fields of paraxial optical vortices," *J. Opt.* **23**(7), 075401 (2021).
22. K. Y. Bliokh and F. Nori, "Transverse and longitudinal angular momenta of light," *Phys. Rep.* **592**, 1–38 (2015).
23. K. Koksai, M. Babiker, V. E. Lembessis, *et al.*, "Truncated optical Bessel modes," *Phys. Rev. A* **105**(6), 063512 (2022).
24. A. Aiello, P. Banzer, M. Neugebauer, *et al.*, "From transverse angular momentum to photonic wheels," *Nat. Photonics* **9**(12), 789–795 (2015).
25. V. E. Lembessis, A. Lyras, and O. M. Aldossary, "Two-level atom dynamics induced by a spin-orbit coupled optical vortex: dressed states formulation," *Opt. Continuum* **2**(5), 1256–1266 (2023).
26. V. E. Lembessis, K. Koksai, J. Yuan, *et al.*, "Chirality-enabled optical dipole potential energy for two-level atoms," *Phys. Rev. A* **103**(1), 013106 (2021).
27. G. F. Quinteiro, C. T. Schmiegelow, D. E. Reiter, *et al.*, "Reexamination of Bessel beams: A generalized scheme to derive optical vortices," *Phys. Rev. A* **99**(2), 023845 (2019).
28. K. Koksai, M. Babiker, V. E. Lembessis, *et al.*, "Hopf index and the helicity of elliptically polarized twisted light," *J. Opt. Soc. Am. B* **39**(2), 459 (2022).
29. S. M. Barnett, F. C. Speirits, and M. Babiker, "Optical angular momentum in atomic transitions: a paradox," *J. Phys. A: Math. Theor.* **55**(23), 234008 (2022).
30. M. Lax, W. H. Louisell, and W. B. McKnight, "From Maxwell to paraxial wave optics," *Phys. Rev. A* **11**(4), 1365–1370 (1975).